

## Article

# First-in-Human Study of [<sup>68</sup>Ga]Ga-NODAGA-E[c(RGDyK)]<sub>2</sub> PET for Integrin $\alpha_v\beta_3$ Imaging in Patients with Breast Cancer and Neuroendocrine Neoplasms: Safety, Dosimetry and Tumor Imaging Ability

Malene Martini Clausen <sup>1,2,3,†</sup>, Esben Andreas Carlsen <sup>1,3,†</sup>, Camilla Christensen <sup>1,3</sup>, Jacob Madsen <sup>1,3</sup>, Malene Brandt-Larsen <sup>1,3</sup>, Thomas Levin Klausen <sup>1,3</sup>, Søren Holm <sup>1,3</sup>, Annika Loft <sup>1,3</sup>, Anne Kiil Berthelsen <sup>1,3</sup>, Niels Kroman <sup>4</sup>, Ulrich Knigge <sup>3,5</sup> and Andreas Kjaer <sup>1,3,\*</sup>



**Citation:** Clausen, M.M.; Carlsen, E.A.; Christensen, C.; Madsen, J.; Brandt-Larsen, M.; Klausen, T.L.; Holm, S.; Loft, A.; Berthelsen, A.K.; Kroman, N.; et al. First-in-Human Study of [<sup>68</sup>Ga]Ga-NODAGA-E[c(RGDyK)]<sub>2</sub> PET for Integrin  $\alpha_v\beta_3$  Imaging in Patients with Breast Cancer and Neuroendocrine Neoplasms: Safety, Dosimetry and Tumor Imaging Ability. *Diagnostics* **2022**, *12*, 851. <https://doi.org/10.3390/diagnostics12040851>

Academic Editor: Hidehiko Okazawa

Received: 14 March 2022

Accepted: 28 March 2022

Published: 30 March 2022

**Publisher's Note:** MDPI stays neutral with regard to jurisdictional claims in published maps and institutional affiliations.



**Copyright:** © 2022 by the authors. Licensee MDPI, Basel, Switzerland. This article is an open access article distributed under the terms and conditions of the Creative Commons Attribution (CC BY) license (<https://creativecommons.org/licenses/by/4.0/>).

- <sup>1</sup> Department of Clinical Physiology and Nuclear Medicine & Cluster for Molecular Imaging, Copenhagen University Hospital—Rigshospitalet & Department of Biomedical Sciences, University of Copenhagen, 2100 Copenhagen, Denmark; malene.martini.clausen@regionh.dk (M.M.C.); esben.andreas.carlsen.01@regionh.dk (E.A.C.); cch@minervaimaging.com (C.C.); jacob.madsen@regionh.dk (J.M.); bdqdk@leo-pharma.com (M.B.-L.); thomas.levin.klausen@regionh.dk (T.L.K.); soeren.holm@regionh.dk (S.H.); annika.loft.jakobsen@regionh.dk (A.L.); anne.kiil.berthelsen@regionh.dk (A.K.B.)
- <sup>2</sup> Department of Oncology, Copenhagen University Hospital—Rigshospitalet, 2100 Copenhagen, Denmark
- <sup>3</sup> ENETS Neuroendocrine Tumor Center of Excellence, Copenhagen University Hospital—Rigshospitalet, 2100 Copenhagen, Denmark; ulrich.peter.knigge@regionh.dk
- <sup>4</sup> Department of Breast Surgery, Copenhagen University Hospital—Herlev/Gentofte Hospital, 2730 Herlev, Denmark; niels.kroman@regionh.dk
- <sup>5</sup> Departments of Clinical Endocrinology and Surgical Gastroenterology, Copenhagen University Hospital—Rigshospitalet, 2100 Copenhagen, Denmark
- \* Correspondence: akjaer@sund.ku.dk
- † These authors contributed equally to this work.

**Abstract:** Arginine-Glycine-Aspartate (RGD)-recognizing cell surface integrins are involved in tumor growth, invasiveness/metastases, and angiogenesis, and are therefore an attractive treatment target in cancers. The subtype integrin  $\alpha_v\beta_3$  is upregulated on endothelial cells during angiogenesis and on tumor cells. In vivo assessment of integrin  $\alpha_v\beta_3$  is possible with positron emission tomography (PET). Preclinical data on radiochemical properties, tumor uptake and radiation exposure identified [<sup>68</sup>Ga]Ga-NODAGA-E[c(RGDyK)]<sub>2</sub> as a promising candidate for clinical translation. In this first-in-human phase I study, we evaluate [<sup>68</sup>Ga]Ga-NODAGA-E[c(RGDyK)]<sub>2</sub> PET in patients with neuroendocrine neoplasms (NEN) and breast cancer (BC). The aim was to investigate safety, biodistribution and dosimetry as well as tracer uptake in tumor lesions. A total of 10 patients (5 breast cancer, 5 neuroendocrine neoplasm) received a single intravenous dose of approximately 200 MBq [<sup>68</sup>Ga]Ga-NODAGA-E[c(RGDyK)]<sub>2</sub>. Biodistribution profile and dosimetry were assessed by whole-body PET/CT performed at 10 min, 1 h and 2 h after injection. Safety assessment with vital parameters, electrocardiograms and blood tests were performed before and after injection. In vivo stability of [<sup>68</sup>Ga]Ga-NODAGA-E[c(RGDyK)]<sub>2</sub> was determined by analysis of blood and urine. PET images were analyzed for tracer uptake in tumors and background organs. No adverse events or pharmacologic effects were observed in the 10 patients. [<sup>68</sup>Ga]Ga-NODAGA-E[c(RGDyK)]<sub>2</sub> exhibited good in vivo stability and fast clearance, primarily by renal excretion. The effective dose was 0.022 mSv/MBq, equaling a radiation exposure of 4.4 mSv at an injected activity of 200 MBq. The tracer demonstrated stable tumor retention and good image contrast. In conclusion, this first-in-human phase I trial demonstrated safe use of [<sup>68</sup>Ga]Ga-NODAGA-E[c(RGDyK)]<sub>2</sub> for integrin  $\alpha_v\beta_3$  imaging in cancer patients, low radiation exposure and favorable uptake in tumors. Further studies are warranted to establish whether [<sup>68</sup>Ga]Ga-NODAGA-E[c(RGDyK)]<sub>2</sub> may become a tool for early identification of patients eligible for treatments targeting integrin  $\alpha_v\beta_3$  and for risk stratification of patients.

**Keywords:** first in human; PET; RGD; breast cancer; neuroendocrine neoplasm; alphavbeta3 integrin

## 1. Introduction

Cell surface adhesion receptors of the integrin superfamily play a fundamental role in physiological as well as pathophysiological processes. The subfamily of Arginine-Glycine-Aspartate (RGD)-recognizing integrins has drawn most attention in the efforts of producing targeting agents due to implications on several of hallmarks of cancer—tumor growth, invasiveness and metastases and angiogenesis [1]. Integrins consist of one alpha and one beta subunit, where the RGD-recognizing integrins are  $\alpha_v\beta_1$ ,  $\alpha_v\beta_3$ ,  $\alpha_v\beta_5$ ,  $\alpha_v\beta_6$ ,  $\alpha_v\beta_8$ ,  $\alpha_5\beta_1$ ,  $\alpha_8\beta_1$  and  $\alpha_{11b}\beta_3$ . Targeting particularly integrin  $\alpha_v\beta_3$  has been pursued due to significant upregulation on activated endothelial cells during angiogenesis, but absence on quiescent endothelial cells [2], thus linking it to neo-angiogenesis. Integrin  $\alpha_v\beta_3$  expression is also seen on tumor cells in certain cancers, and the overexpression of integrin  $\alpha_v\beta_3$  may therefore have implications to several cancer entities, e.g., breast, glioblastoma, and prostate [2].

Initial clinical trials with the  $\alpha_v\beta_3/\alpha_v\beta_5$ -targeting ligand cilengitide showed a modest effect on tumor growth [3,4], while later phase II/phase III trials failed to meet expectations due to unintended pro-angiogenic effects at lower concentrations, and anti-angiogenic effect was seen only at higher concentrations [5]. Recently, new promising pure  $\alpha_v\beta_3$  ligands (TDI-4161 and TDI-3761) have been shown to circumvent the pro-angiogenic effect previously seen with cilengitide [6], hence reinforcing the need for development of methods to assess in vivo the level of  $\alpha_v\beta_3$  integrin expression for selection of patients for such targeted therapies.

A large number of PET tracers with the RGD motif have been developed and tested preclinically. However, only a few have reached testing in clinical trials, and none have yet been employed for routine clinical use. The clinical translation of first-generation integrin-targeting PET tracers with  $^{18}\text{F}$ , e.g.,  $^{18}\text{F}$ -Galacto-RGD, was hampered by complex radiochemistry. Thus, several approaches to optimize the production and tracer stability as well as tumor-binding properties have been investigated [7]. Addressing the need for assessing integrin  $\alpha_v\beta_3$ , our group evaluated a number of PET tracers utilizing cyclic RGD, either as monomer or dimer coupled with  $^{64}\text{Cu}$  or  $^{68}\text{Ga}$  [8–12]. Of these, [ $^{68}\text{Ga}$ ]Ga-NODAGA-E[c(RGDyK)]<sub>2</sub> was found to be particularly promising as it fulfilled the requirements of fast and reliable radiochemical production, imaging abilities, i.e., stable tumor retention and favorable tumor-to-background ratio, favorable human radiation estimates, and was correlated with gene expression of integrin [8–10,13,14]. Furthermore, in vitro assessment of the affinity of NODAGA-E[c(RGDyK)]<sub>2</sub> towards integrin subtype  $\alpha_v\beta_3$  showed an excellent affinity (KD) of 0.075 nM. (Bentsen et al., unpublished data). Taken together, [ $^{68}\text{Ga}$ ]Ga-NODAGA-E[c(RGDyK)]<sub>2</sub> therefore was chosen for human translation.

Here, we present our single-center first-in-human phase I study of the PET tracer [ $^{68}\text{Ga}$ ]Ga-NODAGA-E[c(RGDyK)]<sub>2</sub> in 10 patients with either breast cancer (BC) or neuroendocrine neoplasms (NEN). The primary objective was to evaluate biodistribution, dosimetry and safety and the secondary objective was to assess tumor uptake.

## 2. Materials and Methods

### 2.1. Patients

A total of 10 patients older than 50 years with histopathologically confirmed BC or NEN were enrolled in the phase I study from 24 November 2016 to 26 June 2017. All patients gave written informed consent before inclusion. This study was approved by the Danish Health and Medicine Authority (EudraCT no. 2015-005335-41) and the Regional Scientific Ethical Committee (H-16034365) and registered at ClinicalTrials.gov (NCT02970786). This study was performed in accordance with Good Clinical Practice (GCP), and independently monitored by the GCP unit of the Capital Region of Denmark.

Patients fasted 4 h before intravenous injection of [ $^{68}\text{Ga}$ ]Ga-NODAGA-E[c(RGDyK)]<sub>2</sub> followed by sequential whole-body PET/CT scans. Two peripheral intravenous catheters were placed, one for tracer injection and one in the contralateral arm for withdrawal of blood samples and administration of i.v. contrast agent. Electrocardiogram and vital signs as well as safety blood samples were monitored before and following [ $^{68}\text{Ga}$ ]Ga-NODAGA-E[c(RGDyK)]<sub>2</sub> injection. In a subset of patients, blood samples were collected after [ $^{68}\text{Ga}$ ]Ga-NODAGA-E[c(RGDyK)]<sub>2</sub> injection for pharmacokinetic analyses including ligand stability. Furthermore, urine was collected for pharmacokinetic analysis and dosimetry in a subset of patients (Figure 1).

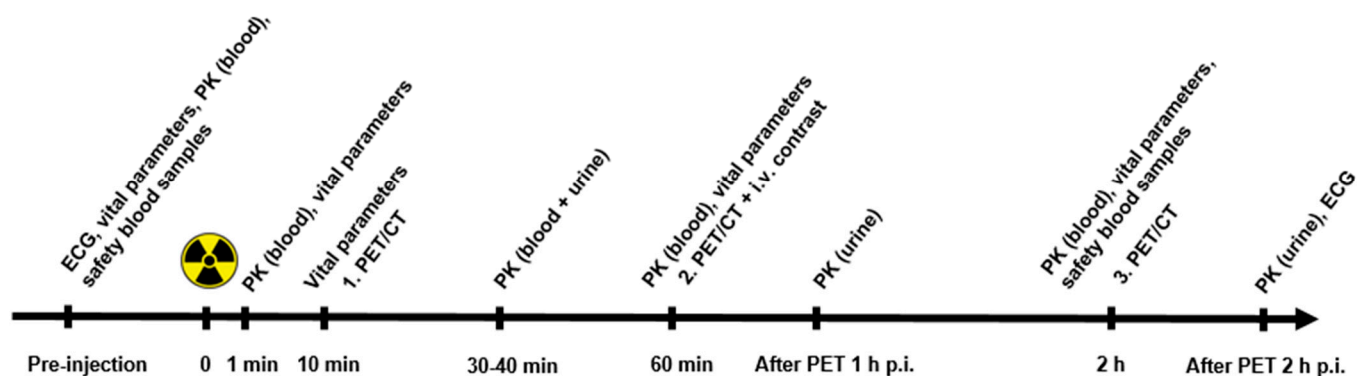


**Figure 1.** Trial events before and after a single-dose injection of [ $^{68}\text{Ga}$ ]Ga-NODAGA-E[c(RGDyK)]<sub>2</sub>. Timeline denotes injection, acquisition of PET/CT imaging, assessment of vital parameters, and collection of blood and urine. Abbreviations: ECG (electrocardiogram), PK (pharmacokinetics), and PET/CT (positron emission tomography).

### 2.2. Synthesis of [ $^{68}\text{Ga}$ ]Ga-NODAGA-E[c(RGDyK)]<sub>2</sub>

NODAGA-E[c(RGDyK)]<sub>2</sub> acetate was obtained from ABX GmbH (Radeberg, Germany). All reagents and cassettes were purchased from Eckert and Ziegler (Berlin, Germany). Gallium-68 ( $T_{1/2} = 68$  min;  $E_{\text{max}}$ ,  $\beta^+ = 1.90$  MeV (89%)) labelling of NODAGA-E[c(RGDyK)]<sub>2</sub> acetate was performed in a Modular-Lab Pharmtracer module (Eckert and Ziegler) using a  $^{68}\text{Ge}/^{68}\text{Ga}$  generator (Galliapharm, 50 mCi, Eckert and Ziegler). The generator was eluted with 6 mL 0.1M HCl. The eluate was concentrated on a Bond Elut SCX cartridge and eluted with 700  $\mu\text{L}$  5M NaCl/5.5M HCl (41:1). NODAGA-E[c(RGDyK)]<sub>2</sub> (50  $\mu\text{g}$ , 30 nmol) was labelled in 1000  $\mu\text{L}$  1.4 M NaOAc buffer pH 4.5 and 400  $\mu\text{L}$  50% EtOH at 60  $^{\circ}\text{C}$  for 300 s. The resulting mixture was transferred to a Sep-pak C2 light cartridge and washed with saline. [ $^{68}\text{Ga}$ ]Ga-NODAGA-E[c(RGDyK)]<sub>2</sub> was eluted with 1 mL 50% EtOH through a sterile filter and formulated with saline. The synthesis time was 20 min and  $533 \pm 167$  MBq [ $^{68}\text{Ga}$ ]Ga-NODAGA-E[c(RGDyK)]<sub>2</sub> was obtained. See Supplementary Material (Section S1) for a description of the quality control.

### 2.3. Plasma Pharmacokinetics and Urine Metabolite Analysis

The activity concentration of the urine and plasma was counted on Cobra II TM Gamma Counter (Packard, CT, USA). Blood and urine samples were analyzed on a Dionex UltiMate 3000 column-switching high-performance liquid chromatography (HPLC) system with a Posi-RAM Module 4 (ThermoFisher Scientific, Waltham, MA, USA). The full blood samples were centrifuged (3500 rpm, 4 min) and the supernatant plasma was collected and filtered through a 0.45  $\mu\text{m}$  syringe filter prior to the HPLC analysis [15]. The HPLC analysis consisted of an extraction step and an analytical step, as previously described [16]. During the extraction step, the plasma samples were passed through a shim-pack XR-ODS (30  $\times$  4.6 mm, 2.2  $\mu\text{m}$ ). The valves were switched, and the sample was then analyzed on an Onyx monolithic column (C18, 50  $\times$  4.6 mm). The mobile phase for the extraction step was 0.1% trifluoroacetic acid (TFA) in H<sub>2</sub>O, while the analytical step was a gradient method with solvent A (0.1% TFA in MeCN:H<sub>2</sub>O 10:90) and solvent B (0.1% TFA in MeCN:H<sub>2</sub>O 90:10),

both with a flow of 1 mL/min. Gradient: 0–6 min (extraction), 6–7 min 5% B, 7–12 min 5–35% B, and 12–14 min 35–5% B.

#### 2.4. PET/CT Acquisition and Image Analysis

Data acquisition was performed using a Biograph mCT PET/CT system (Siemens Medical Solutions, Erlangen, Germany) with an axial field of view of 216 mm. Whole-body PET/CT scans were acquired at 10 min, 1 h and 2 h after intravenous injection of approx. 200 MBq [<sup>68</sup>Ga]Ga-NODAGA-E[c(RGDyK)]<sub>2</sub>. PET/CT scans were obtained in 3D mode with acquisition time of 2 min per bed position (1 min/bed position for lower extremities). A diagnostic CT was obtained before PET 1 h p.i. with a 2 mm slice thickness, 120 kV, and a quality reference of 225 mAs modulated by the Care Dose 4D automatic exposure control system (Siemens Medical Solutions). An automatic injection system was used to administer 75 mL of an iodine-containing contrast agent (Optiray 300; Covidien, Dublin, Ireland) with a scan delay of 60 s and flow rate of 1.5 mL/s, followed by an injection of 150 mL NaCl with a flow rate of 2.5 mL/s. A low-dose CT scan, 2 mm slice thickness, 120 kV, and 40 mAs, was acquired before PET 10 min and PET 2 h p.i., and used for attenuation correction. Using the corresponding CT-scan for attenuation- and scatter correction, the PET data were reconstructed iteratively using the TrueX algorithm including point-spread function and time-of-flight information (Siemens Medical Solutions); the settings were 2 iterations, 21 subsets, 2 mm Gaussian filter, and a 400 × 400 matrix. Pixel size in the final reconstructed PET image was approx. 2 × 2 mm with a slice thickness of 2 mm.

#### 2.5. Tumor Uptake by Visual Image Analysis and Activity Quantification

PET/CT analysis was performed by a team of two experienced board certified specialists in nuclear medicine and radiology, respectively. A volume of interest (VOI) was drawn to encompass the entire lesion on PET images, and standardized uptake values (SUV) for primary and metastatic lesions were registered. If a lesion was not visible on PET, the co-registered CT was used for delineation of the tumor. The lesion in each organ with the highest SUV<sub>max</sub> was reported. Tumor uptake was also qualitatively described as homogeneous or heterogeneous. Tumor size was measured by largest diameter on CT.

#### 2.6. Dosimetry

Dosimetry was based on the decay-uncorrected image sets from the 3 time points (10 patients) supplemented with sampled urine data (7 patients). For each patient, organ, and time point, tissue activity concentration (kBq/mL) was determined in VOIs defined on CT. Activity (per patient, organ and time) was estimated by multiplying concentration values by organ masses of the OLINDA male adult phantom [17], normalized per injected MBq and scaled for patient weight. Time integrated activity coefficients (TIAC, unit h) for each patient and organ was determined by numerical integration and analytical extrapolation to infinity assuming only physical decay. The resulting organ TIACs were averaged over patients. All data were entered into OLINDA/EXM 2.0 software (Vanderbilt University, TN, USA and HERMES Medical Solutions, Stockholm, Sweden) [18].

Urine was collected immediately after each scan in pre-weighted plastic bottles. The cumulated decay-corrected activity (MBq) of the excreted urine was plotted over time for all 7 subjects and data fitted to a one-phase exponential association. The resulting limit and half-life were used as input to the bladder voiding model of OLINDA using a bladder voiding interval of 1 h. A detailed description of the dosimetry is available in Supplementary Material (Section S2).

#### 2.7. Histology

Specimens from primary tumor or metastases were obtained from patients undergoing surgery within four weeks of the PET/CT. The specimens were placed in formalin and paraffin embedded within 24 h. The samples were cut in sections of 4 μM and dewaxed through xylene to tap water. For antigen retrieval the sections were treated with proteinase

K for 5 min. This was followed by a blocking step with Peroxidase-Blocking Solution (Agilent, S2023) and pre-incubation in 2% BSA for 10 min. For visualizing the intensity and distribution of integrin,  $\alpha_v\beta_3$  sections were incubated with primary antibody (Absolute Antibodies, Ab00890-23.0) in a 1:50 dilution in 2% BSA overnight at 40 °C [19].

For visualization, the sections were incubated with Envision+ system Anti-Rabbit (Agilent, K4003) for 45 min followed by incubation with DAB+ system (Agilent, K3468) for 10 min. Counterstaining was performed with Mayer's Hematoxylin. The sections were visually evaluated regarding  $\alpha_v\beta_3$  intensity.

### 2.8. Statistics

Data are presented as the mean with the standard error of mean (SEM) unless otherwise stated. The significance of differences in vital signs and blood tests was evaluated using ANOVA. A  $p$ -value < 0.05 was considered statistically significant.

## 3. Results

### 3.1. Patient Characteristics

Ten patients were included in this study—five patients with NEN and five patients with BC. Patient characteristics are shown in Table 1. All patients were, independently of this study, planned for surgical removal of tumor or metastases subsequent to PET/CT; however, one patient turned out to be unresectable, and one patient had known metastatic disease, and was diagnosed with metastatic spinal cord compression shortly after PET/CT and therefore was not a candidate for surgery.

### 3.2. Radiochemistry

All preparations were within the specifications. The specifications and results of the [ $^{68}\text{Ga}$ ]Ga-NODAGA-E[c(RGDyK)]<sub>2</sub> preparations are listed in Supplemental Table S1.

### 3.3. Patient Safety and Dosimetry

The mean and standard deviation of the administered mass of [ $^{68}\text{Ga}$ ]Ga-NODAGA-E[c(RGDyK)]<sub>2</sub> were  $23.4 \pm 6.4$   $\mu\text{g}$  (range, 12.6–35.8  $\mu\text{g}$ ). The mean and standard deviation of the administered activity were  $184.4 \pm 38.4$  MBq (range, 97.3–220 MBq). There were no adverse or clinically detectable pharmacologic effects in any of the 10 subjects. No significant changes in vital signs or the results of laboratory studies or electrocardiograms were observed (Supplemental Table S2). No acute or long-term effects on blood parameters or organ function were observed during or after this study (Supplemental Figure S1).

The highest radiation dose was received by the urinary bladder wall (0.126 mSv/MBq) followed by the thyroid and kidneys (0.066 and 0.063 mSv/MBq, respectively) (Table 2). The effective dose was 0.022 mSv/MBq or 4.4 mSv for the intended administered activity dose of 200 MBq (mean value for male and female according to ICRP103 [20]).

### 3.4. Biodistribution and Pharmacokinetics

Decay-corrected  $\text{SUV}_{\text{mean}}$  in blood and major organs is plotted individually for all patients in Figure 2. The kidneys were the primary excretion route, whereas only little excretion was observed through the hepatobiliary/gastrointestinal tract. There was a relatively high, but decreasing, activity in the blood pool. Brain, lungs, bone and muscle showed almost no activity.

**Table 1.** Patient characteristics.

Characteristics	Patient No.									
	1	2	3	4	5	6	7	8	9	10
<b>Sex</b>	Male	Male	Female	Female	Male	Female	Female	Female	Female	Male
<b>Age (y)</b>	69	79	55	67	58	58	68	68	63	52
<b>Cancer type</b>	Neuroendocrine	Neuroendocrine	Neuroendocrine	Breast	Neuroendocrine	Breast	Breast	Breast	Breast	Neuroendocrine
<b>Stage/grade</b>	PT in small intestine, metastases in the liver and mesentery	PT in small intestine, metastasis in the mesentery	PT in terminal ileum/coecum	PT left breast	PT not identified, liver metastasis	PT in right breast, SN without metastases	PT in right breast, metastases in 3/14 LN, no distant metastases	PT in left breast, SN without metastases	PT in left breast, SN without metastases	PT in pancreas, liver-, bone, and lymph node metastases
<b>Biomarker status</b>	Ki67 2% *	Ki67 2%	Ki67 1%	ER 100%, HER2 borderline	Ki67 14%	ER 100%, HER2 neg.	ER neg., HER2 neg.	ER 100%, HER2 neg.	ER 100%, HER2 neg.	Ki67 25% *
<b>Concurrent cancer treatment</b>	Lanreotid	Lanreotid	Lanreotid	None	None	None	None	None	None	None
<b>Days from PET scan to biopsy/operation</b>	6	14	30	5	18	6	1	5	5	NA
<b>Tissue</b>	NA	Fresh frozen, later paraffin embedded	Fresh frozen, later paraffin embedded	Paraffin embedded	Paraffin embedded	Paraffin embedded	Paraffin embedded	Paraffin embedded	Paraffin embedded	NA

Abbreviations: ER: estrogen receptor. HER2: human epidermal growth factor receptor 2. LN: lymph node. NA: not available. PT: primary tumor. SN: sentinel node. \* Obtained from biopsy at time of diagnosis.

**Table 2.** [<sup>68</sup>Ga]Ga-NODAGA-E[c(RGDyK)]<sub>2</sub> PET dosimetry.

Organ/Tissue	Mean Absorbed Dose (mGy/MBq)
Adrenals	0.02450
Brain	0.00252
Breasts	0.01050
Esophagus	0.01120
Eyes	0.00929
Gallbladder Wall	0.01430
Left Colon	0.01360
Small Intestine	0.06030
Stomach Wall	0.02630
Right Colon	0.01310
Rectum	0.01510
Heart Wall	0.01460
Kidneys	0.06270
Liver	0.02790
Lungs	0.00792
Ovaries	0.01540
Pancreas	0.01440
Prostate	0.01330
Salivary Glands	0.00996
Red Marrow	0.01500
Osteogenic Cells	0.01360
Spleen	0.05040
Testes	0.01920
Thymus	0.01100
Thyroid	0.06630
Urinary Bladder Wall	0.12600
Uterus	0.01800
Total Body	0.01330
<b>Effective Dose (mSv/MBq)</b>	<b>0.02180</b>

Mean absorbed dose per unit administered activity (mGy/MBq) for major organs was derived from serial whole-body PET scans performed at 10 min, 1 h and 2 h after a single injection of [<sup>68</sup>Ga]Ga-NODAGA-E[c(RGDyK)]<sub>2</sub> using VOI-based time activity data.

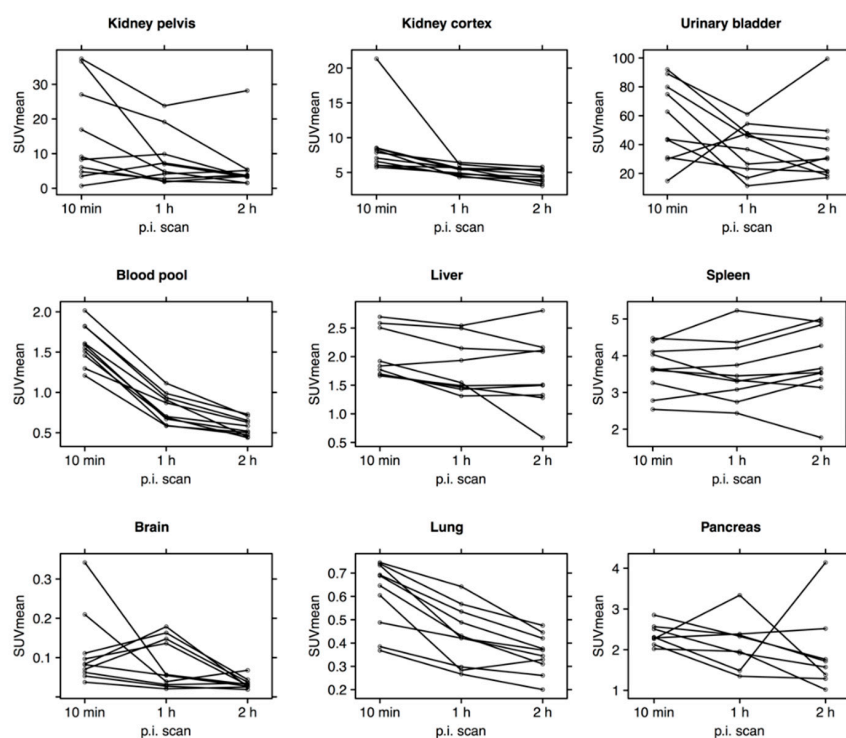


**Figure 2.** Cont.

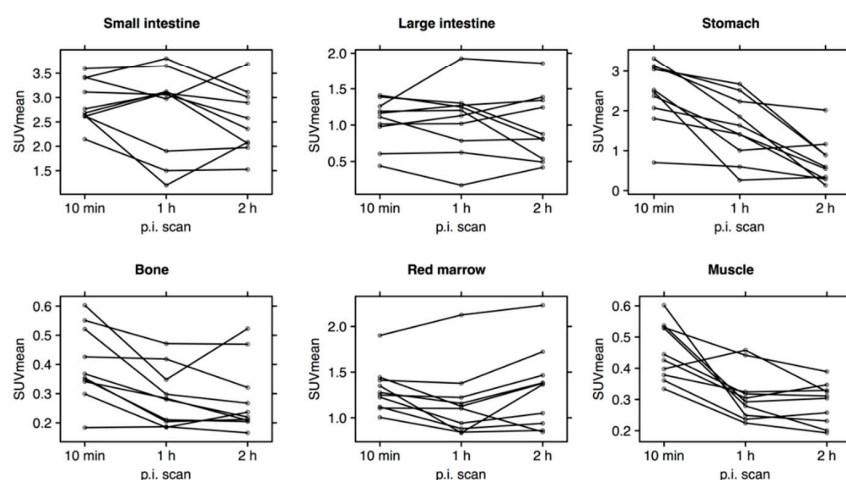


**Figure 2.** SUV<sub>mean</sub> in blood and major organs plotted individually for all patients ( $n = 10$ ). For each patient, VOIs were drawn on selected organs/tissues of interest at all three consecutive PET scans. p.i.: post injection.

Blood and urine from seven patients in this study were used for investigation of the plasma pharmacokinetics of [ $^{68}\text{Ga}$ ]Ga-NODAGA-E[c(RGDyK)]<sub>2</sub>. Time points for PET scans, blood and urine samples are listed in Supplemental Table S3. A plasma half-life of 8.6 min was found and quantitative analysis of plasma with reversed-phase HPLC showed two unknown polar metabolites (Figure 3).

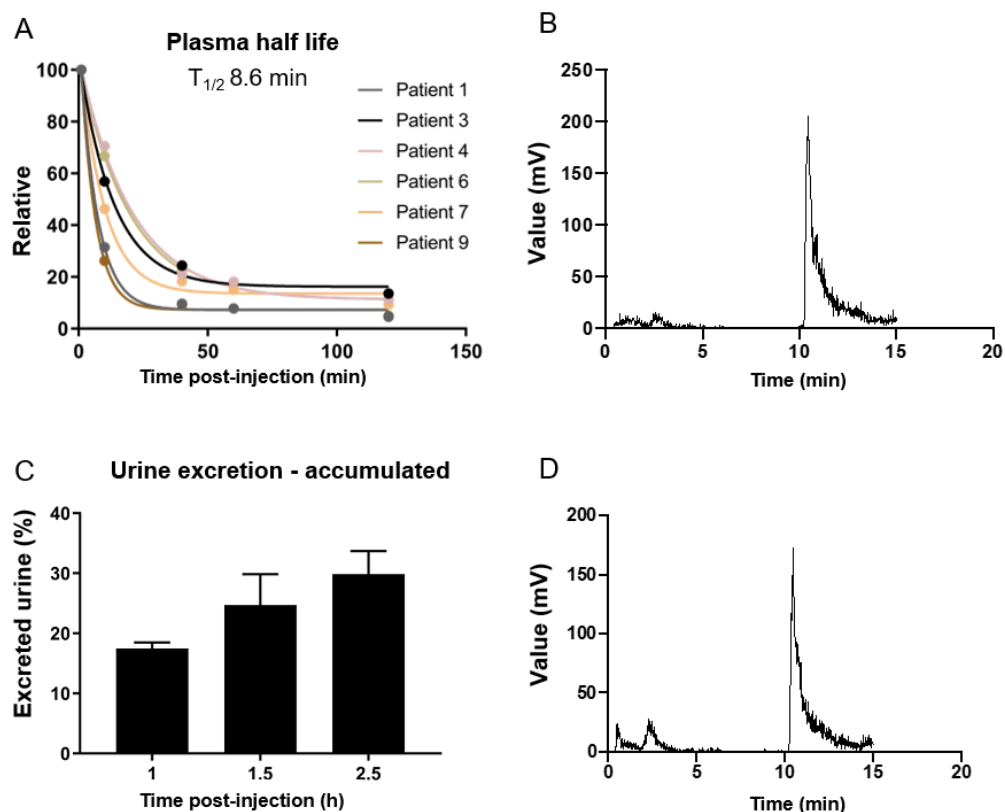


**Figure 3.** (A) Relative time-dependent activity concentrations in plasma. Plasma half-life was estimated to 8.6 min calculated from the half-life from each patient [3.9–14.0 min]. (B) A typical example of a plasma sample 10 min after injection analyzed by HPLC showing two unknown plasma metabolites. (C) Time-dependent excretion of accumulated activity in urine is displayed. (D) A typical example of a urine sample 60 min after injection analyzed by HPLC showing two unknown plasma metabolites.

### 3.5. Tumor Uptake of $[^{68}\text{Ga}]\text{Ga-NODAGA-E}[\text{c}(\text{RGDyK})]_2$ and Target Validation

The tracer demonstrated stable tumor retention and a satisfactory image contrast. On qualitative image analysis, tumors were clearly visualized at the first scan 10 min p.i., and the uptake remained relatively stable over time at the PET 1 and 2 h p.i. (Figure 4). All patients with NEN and BC showed tracer uptake in the primary tumor; however, the amount varied in both disease entities (Table 3). Primary tumor-to-organ ratios are shown in Table 4.

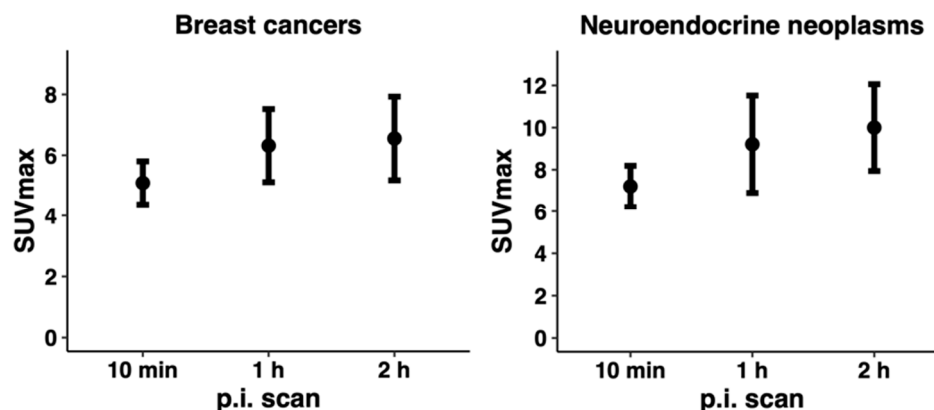


**Figure 4.** Tumor SUV<sub>max</sub>. Mean value of SUV<sub>max</sub> ± SEM for all time points (10 min, 1 h and 2 h p.i.) for breast cancer and neuroendocrine neoplasms is illustrated. A rapid accumulation of tracer was observed, and the uptake remained stable over time.

**Table 3.** Summary of  $[^{68}\text{Ga}]\text{Ga-NODAGA-E}[\text{c}(\text{RGDyK})]_2$  PET/CT.

Patient No.	Tumor Type	Tumor Size	Qualitative PET Uptake	SUV <sub>max</sub>			SUV <sub>mean</sub>		
				PET <sub>10</sub>	PET <sub>1h</sub>	PET <sub>2h</sub>	PET <sub>10</sub>	PET <sub>1h</sub>	PET <sub>2h</sub>
1	NEN	4.4 cm	Heterogeneous	4.53	4.55	5.70	2.58	2.37	2.93
2	NEN	4.9 cm	Heterogeneous	10.36	17.70	14.32	5.31	8.74	7.73
3	NEN	4.4 cm	Heterogeneous	7.85	8.77	15.35	4.10	4.48	7.86
4	BC	6 cm	Heterogeneous	6.18	8.75	10.53	3.26	4.52	5.44
5	NEN	16 cm *	Heterogeneous	7.39	9.39	8.83	2.93	3.2	3.15
6	BC	1.1 cm	Homogeneous	4.88	7.15	8.02	4.59	6.75	6.79
7	BC	1.4 cm	Homogeneous	3.05	2.29	2.66	1.67	1.30	1.94
8	BC	1.8 cm	Homogeneous	7.09	8.40	7.10	4.18	4.70	4.04
9	BC	0.9 cm	Homogeneous	4.24	4.99	4.45	2.36	2.54	2.58
10	NEN	10 cm	Heterogeneous	5.90	7.58	5.80	3.27	3.69	3.05

Readouts of primary tumor SUV<sub>max</sub> and SUV<sub>mean</sub> for all patients at all time points. Tumor size is based on the largest diameter of primary tumor on CT. \* SUV<sub>max</sub>/SUV<sub>mean</sub> values and tumor size of liver metastasis as location of primary neuroendocrine tumor was unknown. BC: breast cancer. NEN: neuroendocrine neoplasm PET<sub>10</sub>: PET 10 min after injection. PET<sub>1h</sub>: PET 1 h after injection. PET<sub>2h</sub>: PET 2 h after injection.

**Table 4.** Tumor-to-organ ratios for patients with breast cancer or neuroendocrine neoplasms.

	PET 10 min p.i.			PET 1 h p.i.			PET 2 h p.i.		
	BC	NEN	All	BC	NEN	All	BC	NEN	All
Tumor to blood	2.79 (0.45)	3.96 (0.61)	3.37 (0.40)	5.72 (1.27)	9.40 (2.06)	7.56 (1.30)	12.1 (4.11)	11.4 (1.81)	11.7 (2.12)
Tumor to liver	2.37 (0.43)	2.58 (0.30)	2.48 (0.25)	3.18 (0.67)	3.21 (0.69)	3.20 (0.45)	2.67 (0.55)	2.89 (0.36)	2.78 (0.31)
Tumor to kidney	0.60 (0.14)	0.81 (0.16)	0.70 (0.11)	1.07 (0.24)	1.48 (0.26)	1.27 (0.18)	1.08 (0.23)	1.56 (0.24)	1.32 (0.18)
Tumor to muscle	7.11 (1.42)	10.2 (1.81)	8.64 (1.20)	11.9 (4.36)	15.5 (4.08)	13.7 (2.88)	7.40 (2.68)	11.4 (3.35)	9.42 (2.13)

Tumor-to-organ ratios (Tumor lesion SUV<sub>max</sub>/Organ SUV<sub>mean</sub>) are shown as the mean (standard error of mean). All: BC + NEN; BC: breast cancer (n = 5); NEN: neuroendocrine neoplasm (n = 5); p.i.: post injection.

Due to the low background uptake in the normal breast tissue, the primary tumors in patients with BC were visualized clearly, whereas the intestine displayed a slightly higher

background uptake for imaging of NEN (Figures 5 and 6). In general, BC displayed a homogeneous tumor uptake of [ $^{68}\text{Ga}$ ]Ga-NODAGA-E[c(RGDyK)]<sub>2</sub>, while NEN demonstrated a more heterogeneous uptake.

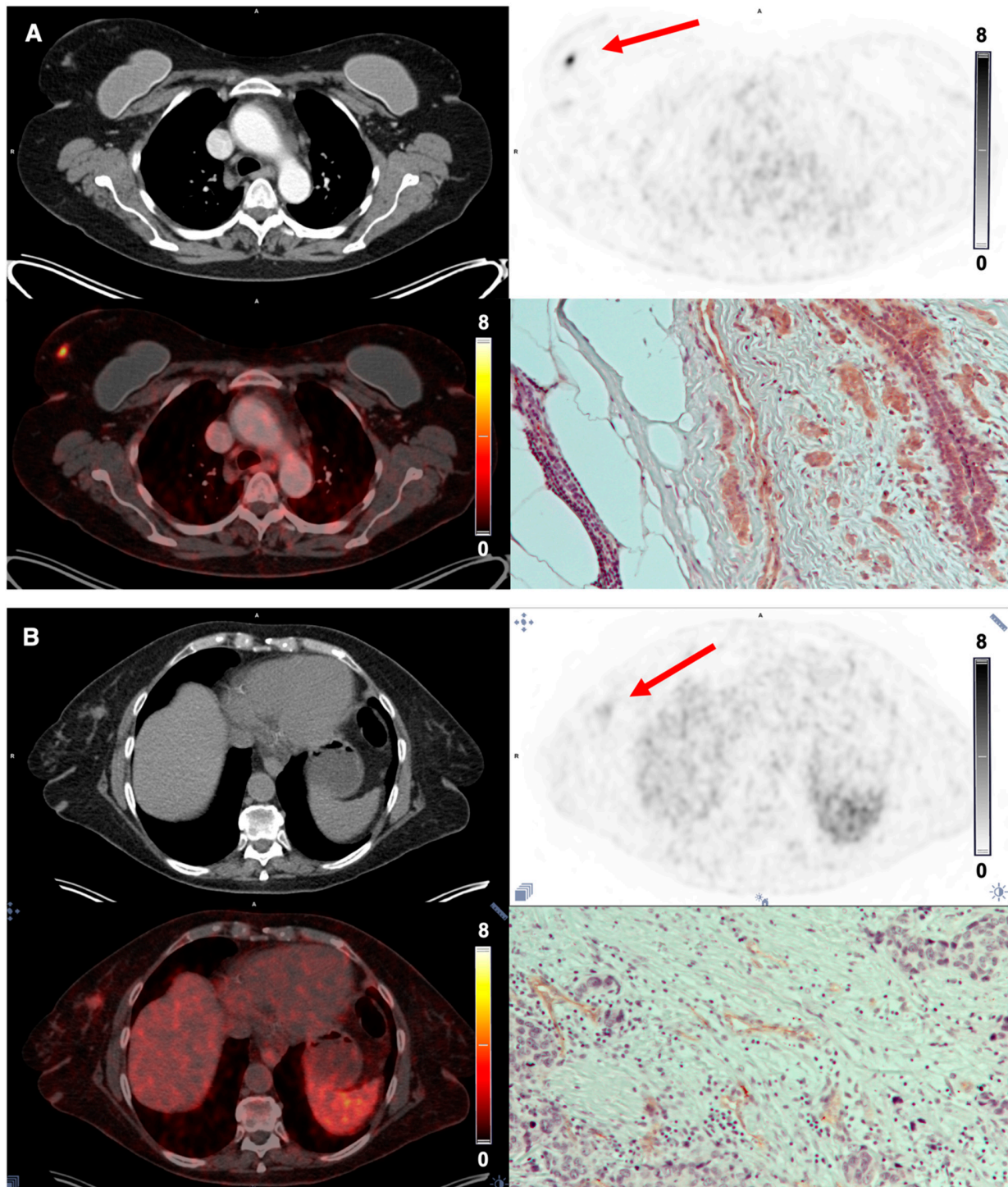


**Figure 5.** [ $^{68}\text{Ga}$ ]Ga-NODAGA-E[c(RGDyK)]<sub>2</sub> PET imaging in breast cancer. (A) Representative transverse CT, PET (1 h p.i.) and fused PET/CT images of primary tumor lesion (red arrow) with a high uptake of [ $^{68}\text{Ga}$ ]Ga-NODAGA-E[c(RGDyK)]<sub>2</sub> (patient 6) and immunohistochemistry staining for integrin  $\alpha_v\beta_3$  in primary tumor showing intense staining. (B) CT, PET (1 h p.i.) and PET/CT of primary tumor lesion with a low uptake of tracer (patient 7) and immunohistochemistry staining confirming low intensity of integrin  $\alpha_v\beta_3$  staining.

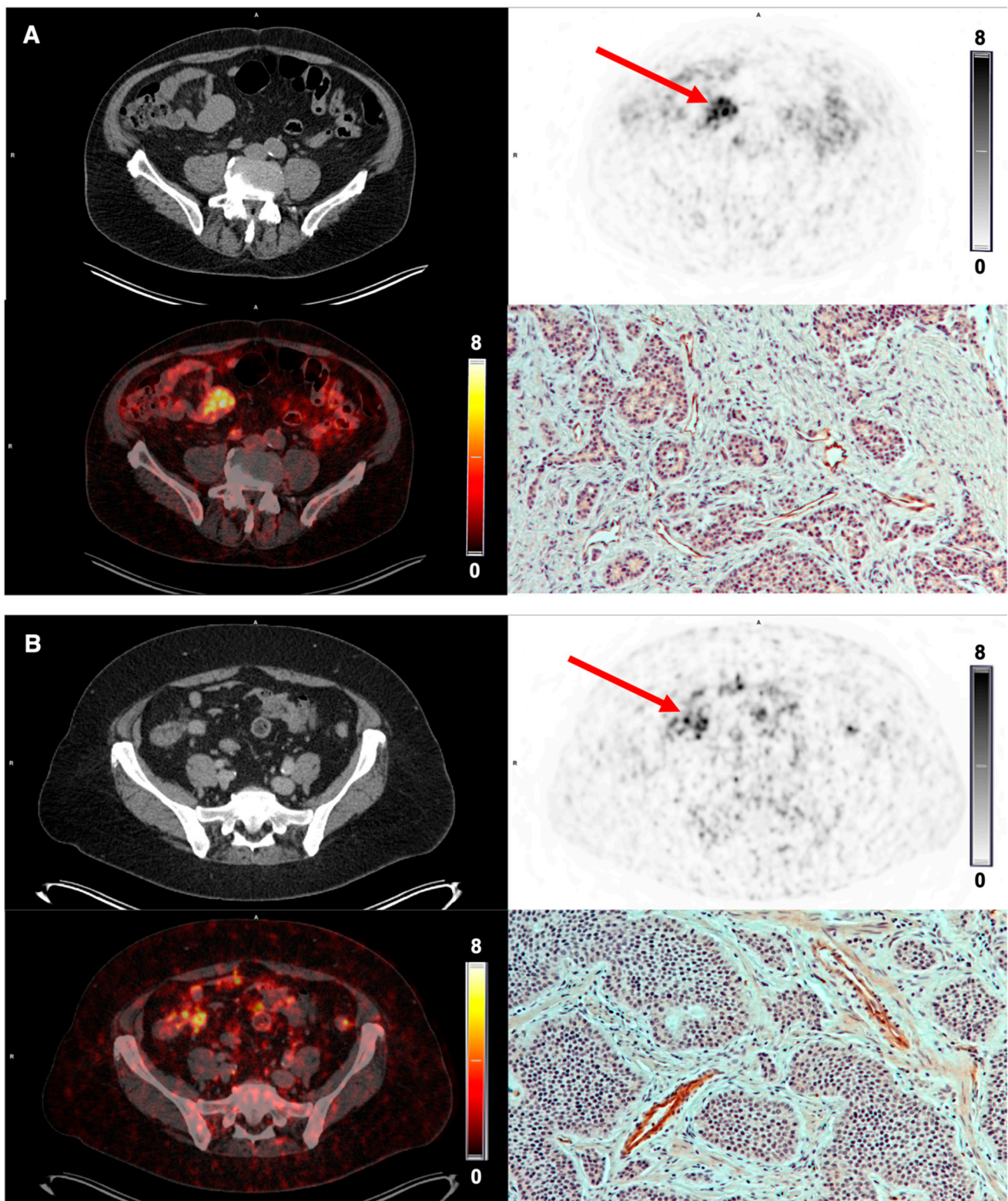


**Figure 6.**  $[^{68}\text{Ga}]\text{Ga-NODAGA-E}[\text{c}(\text{RGDyK})]_2$  PET imaging in NET. (A) Representative transverse CT, PET (1 h p.i.) and fused PET/CT images of primary tumor lesion (red arrow) with a high uptake of  $[^{68}\text{Ga}]\text{Ga-NODAGA-E}[\text{c}(\text{RGDyK})]_2$  in small intestine primary tumor (patient 2) and high intensity immunohistochemistry staining for integrin  $\alpha_v\beta_3$ . (B) Patient 3 also displays a high uptake of tracer in the terminal ileum primary tumor and a corresponding high intensity of integrin  $\alpha_v\beta_3$  immunohistochemistry staining.

A gradual increase in integrin  $\alpha_v\beta_3$ -stained blood vessels and tumor cells was seen with increasing tracer uptake, i.e., increasing  $SUV_{max}/SUV_{mean}$  for both BC and NEN. In Figures 5 and 6, PET images and IHC staining intensity in two patients with BC and two patients with NEN are shown. PET images for the remaining patients are available in Supplemental Figure S2.

#### 4. Discussion

Here, we present the results of our first-in-human phase I study evaluating the safety, biodistribution and dosimetry of [ $^{68}\text{Ga}$ ]Ga-NODAGA-E[c(RGDyK)]<sub>2</sub> PET imaging of integrin  $\alpha_v\beta_3$  in patients with NEN or BC. [ $^{68}\text{Ga}$ ]Ga-NODAGA-E[c(RGDyK)]<sub>2</sub> imaging was safe and no adverse events were observed. Patients did not report any changes in well-being, and no significant changes in vital parameters, electrocardiogram or blood tests (hematology, liver and kidney function) were registered. Biodistribution analysis showed that the kidneys were the primary excretion route, and that hepatobiliary excretion was limited. The effective dose was 0.022 mSv/MBq equaling 4.4 mSv at an injected activity of 200 MBq. Thus, the effective dose is less than the effective dose that is received from a standard  $^{18}\text{F}$ -FDG PET scan [21].

A secondary objective of our study was to assess [ $^{68}\text{Ga}$ ]Ga-NODAGA-E[c(RGDyK)]<sub>2</sub> uptake in tumors. We observed a higher tracer uptake at all imaging time points in NENs, with a mean  $SUV_{max}$  7.21 (10 min p.i., range 4.53–10.36), 9.60 (1 h p.i., range 4.55–17.70) and 10.00 (2 h p.i., range 5.70–15.35), whereas the mean  $SUV_{max}$  in BC was 5.09 (10 min p.i., range 3.05–7.09), 6.32 (1 h p.i., range 2.29–8.75) and 6.55 (2 h p.i., range 2.66–10.53). In both cancer types, we observed a continually increased tumor uptake within the first hour leveling off and stabilizing thereafter, indicating a favorable time point for imaging at 1 h p.i. This was also the case regarding tumor-to-organ ratios, where tumor-to-muscle and tumor-to-liver ratios peaked at 1 h p.i. BC seemed to display a homogeneous tracer uptake, whereas the uptake in NEN was more heterogeneous. However, this may partly be explained by variation in tumor size as the cases with BC and NEN display a median tumor size of 1.4 cm (range 0.9–6.0 cm) and 4.9 (range 4.4–16.0 cm), respectively. Additionally, target validation by comparison of tumor uptake of [ $^{68}\text{Ga}$ ]Ga-NODAGA-E[c(RGDyK)]<sub>2</sub> and tissue expression of integrin  $\alpha_v\beta_3$  was performed. By visual analysis, a correlation between the intensity of integrin  $\alpha_v\beta_3$  staining and tracer uptake was observed. The staining intensity was evaluated visually since no formal scoring system for integrin  $\alpha_v\beta_3$  staining has been developed and due to the low number of patients. Additionally evident from the integrin  $\alpha_v\beta_3$  staining is the fact that  $\alpha_v\beta_3$  is expressed at both newly formed vessels, but also tumor cells. This is in line with previously published immunohistochemical data showing that  $\alpha_v\beta_3$  is indeed expressed on endothelium of neo-vessels as well as on tumor cells [2]. Comparison with other RGD-based PET tracers is complicated by the small sample size of this and other studies, as well as differences in the type of cancer investigated, disease stage and treatments. Previously, other clinically tested PET tracers have reported predominantly renal clearance and moderate tracer uptake in liver, spleen, and intestines [22]. The data presented here for [ $^{68}\text{Ga}$ ]Ga-NODAGA-E[c(RGDyK)]<sub>2</sub> are in line with this, i.e., predominantly renal clearance and moderate uptake in liver, spleen and intestines. When comparing the uptake of PET tracers in tumors, the uptake varies both within the same cancer entities as well as between different cancer entities. In the largest study of BC ( $n = 42$ ), the dimeric RGD-based PET tracer  $^{18}\text{F}$ -Alfatide II had a mean  $SUV_{max}$  of  $3.77 \pm 1.78$  [23]. In the current study, we found a numerically higher tracer uptake in patients with BC (mean  $SUV_{max}$  of 6.2 at 1 h p.i.). In our study, patient no. 7 had a triple-negative BC with regional lymph node metastases. Surprisingly, this tumor displayed a low tracer uptake, whereas patient no. 6 with a localized ER and HER2-positive tumor had a high tracer uptake. This was also observed for  $^{18}\text{F}$ -Alfatide II [23]. To the best of our knowledge, imaging of patients with NEN with RGD tracers has not been reported previously, although different combined tracers with, e.g., RGD and a somatostatin analog have been reported [24]. Multimerization of the RGD motif increases binding avidity, while

also increasing radiation of the kidneys due to renal retention [7]. Recently, a study of 10 patients with head and neck squamous cell carcinoma reported mean  $SUV_{max}$  of  $3.9 \pm 1.1$  in the primary tumor when applying the monomeric [ $^{68}Ga$ ]Ga-NODAGA-RGDyK [25]. A dosimetry analysis showed an effective dose of 19.8  $\mu Sv/MBq$  and kidney radiation of 0.046 mGy/MBq [26] in comparison with an effective dose of 22  $\mu Sv/MBq$  and kidney radiation of 0.063 mGy/MBq present in the current study.

Overall, the data of the current phase I trial are encouraging for proceeding with additional testing of [ $^{68}Ga$ ]Ga-NODAGA-E[c(RGDyK)]<sub>2</sub> for in vivo whole-body assessment of integrin  $\alpha_v\beta_3$  and evaluation of possible clinical implications. While cilengitide targeting  $\alpha_v\beta_3/\alpha_v\beta_5$  revealed a dose-dependent effect with an unintended pro-angiogenic effects at lower concentrations, leading to the overall failure in large trials, newer specific  $\alpha_v\beta_3$  ligands (TDI-3761 and TDI-4161) have shown promising results [6]. Our data underline the varying degree of  $\alpha_v\beta_3$  expression between different cancers, in *casu* BC and NEN. Furthermore, patients that may present with similar disease state based on routine clinical biomarkers, e.g., Ki67% and ER/HER2 receptor status, can show large variation in  $\alpha_v\beta_3$  expression. Accordingly, e.g., patients no. 1 and 2 both had an approximately 4 cm primary NEN in the small intestine, metastatic disease and a Ki67 index of 2%. However, although comparable clinical characteristics, patient no. 2 exhibited the highest  $SUV_{max}$  among all of the NEN patients at all time points ( $SUV_{max}$ : 10.36–17.70), whereas patient no. 1 had the lowest  $SUV_{max}$  ( $SUV_{max}$ : 4.53–5.70). This underscores that in future clinical trials of new selective  $\alpha_v\beta_3$ -targeting therapies, patient selection with companion diagnostics  $\alpha_v\beta_3$  integrin imaging may be important to enroll only patients with high levels of integrin expression, thus improving the likelihood of demonstrating a treatment effect. Ultimately, [ $^{68}Ga$ ]Ga-NODAGA-E[c(RGDyK)]<sub>2</sub> PET may therefore guide decisions on treatments targeting integrin  $\alpha_v\beta_3$  as well as follow-up for monitoring response to treatment [27]. Furthermore, given the relationship between integrin  $\alpha_v\beta_3$  and tumor growth, invasion/metastasis, and angiogenesis, risk stratification of patients may also become possible by means of [ $^{68}Ga$ ]Ga-NODAGA-E[c(RGDyK)]<sub>2</sub> PET [2].

## 5. Conclusions

Based on the present phase I study, we conclude that PET imaging with the tracer [ $^{68}Ga$ ]Ga-NODAGA-E[c(RGDyK)]<sub>2</sub> is safe and well tolerated. The tracer exhibited a low effective dose and good imaging contrast with variable tumor uptake in NEN and BC probably reflecting inter-individual differences in expression of integrin  $\alpha_v\beta_3$ . We suggest that the PET tracer may become a promising tool for early identification of patients eligible for treatments targeting integrin  $\alpha_v\beta_3$  and for risk stratification of patients.

## 6. Patents

Malene Brandt-Larsen, Jacob Madsen and Andreas Kjaer are inventors/hold IPR on a patent application: “ $^{68}Ga$ - and  $^{64}Cu$ -NODAGA-E[c(RGDyK)]<sub>2</sub> for use as pet tracers in the imaging of angiogenesis in humans” (WO2019091534A1). No other potential conflicts of interest relevant to this article exist.

**Supplementary Materials:** The following supporting information can be downloaded at: <https://www.mdpi.com/article/10.3390/diagnostics12040851/s1>. References [17,18,20] are cited in the supplementary materials. Description of Section S1 quality control of [ $^{68}Ga$ ]Ga-NODAGA-E[c(RGDyK)]<sub>2</sub> and Section S2 dosimetry; Figure S1: Laboratory tests before and after injection of [ $^{68}Ga$ ]Ga-NODAGA-E[c(RGDyK)]<sub>2</sub>; Figure S2: [ $^{68}Ga$ ]Ga-NODAGA-E[c(RGDyK)]<sub>2</sub> PET/CT images; Table S1: Specifications and results of the [ $^{68}Ga$ ]Ga-NODAGA-E[c(RGDyK)]<sub>2</sub> preparations; Table S2: Vital parameters during PET scans; Table S3: Time points for PET scans, blood and urine samples.

**Author Contributions:** M.M.C.: protocol, patient inclusion, data curation, formal analysis, project administration, and writing—original draft; E.A.C.: data curation, formal analysis, and writing—original draft; C.C.: tracer production, pharmacokinetics and metabolite analysis, and writing—original draft (radiochemistry part); J.M.: pharmacokinetics and metabolite analysis, and writing—

original draft (radiochemistry part); M.B.-L.: tracer production, writing—original draft (radiochemistry part), and writing—review and editing; T.L.K.: biodistribution and dosimetry, and writing—original draft (dosimetry part); S.H.: biodistribution and dosimetry, and writing—original draft (dosimetry part); A.L.: PET/CT image analysis, and writing—review and editing; A.K.B.: PET/CT image analysis, and writing—review and editing; N.K.: patient inclusion, and writing—review and editing; U.K.: patient inclusion, and writing—review and editing; A.K.: conceptualization, methodology, data curation, formal analysis, supervision, and writing—review and editing. All authors have read and agreed to the published version of the manuscript.

**Funding:** This research was funded by the European Union’s Horizon 2020 research and innovation programme under grant agreements no. 670261 (ERC Advanced Grant) and 668532 (Click-It), the Lundbeck Foundation, the Novo Nordisk Foundation, the Innovation Fund Denmark, the Danish Cancer Society, Arvid Nilsson Foundation, the Neye Foundation, the Research Foundation of Rigshospitalet, the Danish National Research Foundation (grant 126), the Research Council of the Capital Region of Denmark, the Danish Health Authority, the John and Birthe Meyer Foundation and Research Council for Independent Research. Andreas Kjaer is a Lundbeck Foundation Professor.

**Institutional Review Board Statement:** This study was conducted in accordance with the Declaration of Helsinki and this study was approved by the Danish Health and Medicine Authority (EudraCT no. 2015-005335-41) and the Regional Scientific Ethical Committee (H-16034365) and registered at ClinicalTrials.gov (NCT02970786). This study was performed in accordance with Good Clinical Practice (GCP), and independently monitored by the GCP unit of the Capital Region of Denmark.

**Informed Consent Statement:** Informed consent was obtained from all subjects involved in this study.

**Data Availability Statement:** Data are not publicly available due to protection of personal data and medical confidentiality.

**Acknowledgments:** We are grateful to the staff at the Department of Clinical Physiology and Nuclear Medicine for invaluable assistance with performing the PET/CT studies and for the patients for participating in this study.

**Conflicts of Interest:** Malene Brandt-Larsen, Jacob Madsen and Andreas Kjaer are inventors/holds IPR on a patent application: “<sup>68</sup>Ga- and <sup>64</sup>Cu-nodaga-e[*rgdyk*]<sub>2</sub> for use as pet tracers in the imaging of angiogenesis in humans” (WO2019091534A1). No other potential conflicts of interest relevant to this article exist. The other authors declare no conflict of interest. The funders had no role in the design of the study; in the collection, analyses, or interpretation of data; in the writing of the manuscript, or in the decision to publish the results.

## References

1. Ludwig, B.S.; Kessler, H.; Kossatz, S.; Reuning, U. RGD-Binding Integrins Revisited: How Recently Discovered Functions and Novel Synthetic Ligands (Re-)Shape an Ever-Evolving Field. *Cancers* **2021**, *13*, 1711. [[CrossRef](#)] [[PubMed](#)]
2. Nieberler, M.; Reuning, U.; Reichart, F.; Notni, J.; Wester, H.J.; Schwaiger, M.; Weinmuller, M.; Rader, A.; Steiger, K.; Kessler, H. Exploring the Role of RGD-Recognizing Integrins in Cancer. *Cancers* **2017**, *9*, 116. [[CrossRef](#)]
3. Nabors, L.B.; Mikkelsen, T.; Hegi, M.E.; Ye, X.; Batchelor, T.; Lesser, G.; Peereboom, D.; Rosenfeld, M.R.; Olsen, J.; Brem, S.; et al. A safety run-in and randomized phase 2 study of cilengitide combined with chemoradiation for newly diagnosed glioblastoma (NABTT 0306). *Cancer* **2012**, *118*, 5601–5607. [[CrossRef](#)]
4. Reardon, D.A.; Fink, K.L.; Mikkelsen, T.; Cloughesy, T.F.; O’Neill, A.; Plotkin, S.; Glantz, M.; Ravin, P.; Raizer, J.J.; Rich, K.M.; et al. Randomized Phase II Study of Cilengitide, an Integrin-Targeting Arginine-Glycine-Aspartic Acid Peptide, in Recurrent Glioblastoma Multiforme. *J. Clin. Oncol.* **2008**, *26*, 5610–5617. [[CrossRef](#)] [[PubMed](#)]
5. Stupp, R.; Hegi, M.E.; Gorlia, T.; Erridge, S.C.; Perry, J.; Hong, Y.-K.; Aldape, K.D.; Lhermitte, B.; Pietsch, T.; Grujicic, D.; et al. Cilengitide combined with standard treatment for patients with newly diagnosed glioblastoma with methylated MGMT promoter (CENTRIC EORTC 26071-22072 study): A multicentre, randomised, open-label, phase 3 trial. *Lancet Oncol.* **2014**, *15*, 1100–1108. [[CrossRef](#)]
6. Li, J.; Fukase, Y.; Shang, Y.; Zou, W.; Muñoz-Félix, J.M.; Buitrago, L.; van Agthoven, J.; Zhang, Y.; Hara, R.; Tanaka, Y.; et al. Novel Pure  $\alpha$ V $\beta$ 3 Integrin Antagonists That Do Not Induce Receptor Extension, Prime the Receptor, or Enhance Angiogenesis at Low Concentrations. *ACS Pharmacol. Transl. Sci.* **2019**, *2*, 387–401. [[CrossRef](#)] [[PubMed](#)]
7. Liolios, C.; Sachpekidis, C.; Kolocouris, A.; Dimitrakopoulou-Strauss, A.; Bouziotis, P. PET Diagnostic Molecules Utilizing Multimeric Cyclic RGD Peptide Analogs for Imaging Integrin  $\alpha$ V $\beta$ 3 Receptors. *Molecules* **2021**, *26*, 1792. [[CrossRef](#)] [[PubMed](#)]

8. Oxboel, J.; Brandt-Larsen, M.; Madsen, J.; Kjaer, A. Uptake of the Angiogenesis PET Tracer  $^{68}\text{Ga}$ -NODAGA-E[c(RGDyK)]<sub>2</sub> Correlates Strongly with Angiopoietin-1 and Angiopoietin-2 Expression in Human Neuroendocrine Xenograft Tumors in Mice. *J. Nucl. Med.* **2016**, *57*, 1367.
9. Oxboel, J.; Brandt-Larsen, M.; Schjoeth-Eskesen, C.; Myschetzky, R.; El-Ali, H.H.; Madsen, J.; Kjaer, A. Comparison of two new angiogenesis PET tracers  $^{68}\text{Ga}$ -NODAGA-E[c(RGDyK)]<sub>2</sub> and  $^{64}\text{Cu}$ -NODAGA-E[c(RGDyK)]<sub>2</sub>; in vivo imaging studies in human xenograft tumors. *Nucl. Med. Biol.* **2014**, *41*, 259–267. [[CrossRef](#)]
10. Brandt-Larsen, M.; Oxboel, J.; Kjaer, A.; Madsen, J. Synthesis and evaluation of  $^{68}\text{Ga}$ -NODAGA-E[c(RGDyK)]<sub>2</sub>. *J. Label. Compd. Radiopharm.* **2013**, *56*, S205.
11. Oxboel, J.; Schjoeth-Eskesen, C.; Madsen, J.; El Ali, H.; Kjaer, A. Strong correlation between  $^{64}\text{Cu}$ -NODAGA-RGD uptake and quantitative gene expression of integrin- $\alpha\text{V}\beta\text{3}$  in human neuroendocrine tumor xenografts in mice. *J. Nucl. Med.* **2012**, *53*, 1101.
12. Oxboel, J.; Schjoeth-Eskesen, C.; El-Ali, H.H.; Madsen, J.; Kjaer, A.  $^{64}\text{Cu}$ -NODAGA-c(RGDyK) Is a Promising New Angiogenesis PET Tracer: Correlation between Tumor Uptake and Integrin  $\alpha\text{V}\beta\text{3}$  Expression in Human Neuroendocrine Tumor Xenografts. *Int. J. Mol. Imaging* **2012**, *2012*, 379807. [[CrossRef](#)] [[PubMed](#)]
13. Clemmensen, A.; Hansen, A.E.; Holst, P.; Schøier, C.; Bisgaard, S.; Johannesen, H.H.; Ardenkjær-Larsen, J.H.; Kristensen, A.T.; Kjaer, A. [ $^{68}\text{Ga}$ ]Ga-NODAGA-E[(cRGDyK)]<sub>2</sub> PET and hyperpolarized [1- $^{13}\text{C}$ ] pyruvate MRSI (hyperPET) in canine cancer patients: Simultaneous imaging of angiogenesis and the Warburg effect. *Eur. J. Nucl. Med. Mol. Imaging* **2020**, *48*, 395–405. [[CrossRef](#)] [[PubMed](#)]
14. Bentsen, S.; Clemmensen, A.; Loft, M.; Flethoj, M.; Debes, K.P.; Ludvigsen, T.P.; Larsen, C.B.; Kirchhoff, J.; Olsen, L.H.; Moller, J.E.; et al. [ $^{68}\text{Ga}$ ]Ga-NODAGA-E[(cRGDyK)]<sub>2</sub> Angiogenesis PET/MR in a Porcine Model of Chronic Myocardial Infarction. *Diagnostics* **2021**, *11*, 1807. [[CrossRef](#)]
15. Hansen, H.D.; Etrup, A.; Herth, M.M.; Dyssegaard, A.; Ratner, C.; Gillings, N.; Knudsen, G.M. Direct comparison of [ $^{18}\text{F}$ ]MH.MZ and [ $^{18}\text{F}$ ]altanserin for 5-HT<sub>2A</sub> receptor imaging with PET. *Synapse* **2013**, *67*, 328–337. [[CrossRef](#)] [[PubMed](#)]
16. Gillings, N. A restricted access material for rapid analysis of [ $^{11}\text{C}$ ]-labeled radiopharmaceuticals and their metabolites in plasma. *Nucl. Med. Biol.* **2009**, *36*, 961–965. [[CrossRef](#)] [[PubMed](#)]
17. Stabin, M.G.; Siegel, J.A. Physical models and dose factors for use in internal dose assessment. *Health Phys.* **2003**, *85*, 294–310. [[CrossRef](#)]
18. Stabin, M.G.; Siegel, J.A. RADAR Dose Estimate Report: A Compendium of Radiopharmaceutical Dose Estimates Based on OLINDA/EXM Version 2.0. *J. Nucl. Med.* **2018**, *59*, 154–160. [[CrossRef](#)]
19. Goodman, S.L.; Grote, H.J.; Wilm, C. Matched rabbit monoclonal antibodies against alphav-series integrins reveal a novel  $\alpha\text{v}\beta\text{3}$ -LIBS epitope, and permit routine staining of archival paraffin samples of human tumors. *Biol. Open* **2012**, *1*, 329–340. [[CrossRef](#)] [[PubMed](#)]
20. *The 2007 Recommendations of the International Commission on Radiological Protection*; ICRP Publication: Stockholm, Switzerland, 2007; Volume 37. [[CrossRef](#)]
21. Quinn, B.; Dauer, Z.; Pandit-Taskar, N.; Schoder, H.; Dauer, L.T. Radiation dosimetry of 18F-FDG PET/CT: Incorporating exam-specific parameters in dose estimates. *BMC Med. Imaging* **2016**, *16*, 41. [[CrossRef](#)]
22. Chen, H.; Niu, G.; Wu, H.; Chen, X. Clinical Application of Radiolabeled RGD Peptides for PET Imaging of Integrin  $\alpha\text{v}\beta\text{3}$ . *Theranostics* **2016**, *6*, 78–92. [[CrossRef](#)]
23. Wu, J.; Wang, S.; Zhang, X.; Teng, Z.; Wang, J.; Yung, B.C.; Niu, G.; Zhu, H.; Lu, G.; Chen, X.  $^{18}\text{F}$ -Alfatide II PET/CT for Identification of Breast Cancer: A Preliminary Clinical Study. *J. Nucl. Med.* **2018**, *59*, 1809–1816. [[CrossRef](#)] [[PubMed](#)]
24. Zheng, Y.; Wang, H.; Tan, H.; Cui, X.; Yao, S.; Zang, J.; Zhang, L.; Zhu, Z. Evaluation of Lung Cancer and Neuroendocrine Neoplasm in a Single Scan by Targeting Both Somatostatin Receptor and Integrin  $\alpha\text{v}\beta\text{3}$ . *Clin. Nucl. Med.* **2019**, *44*, 687–694. [[CrossRef](#)]
25. Durante, S.; Dunet, V.; Gorostidi, F.; Mitsakis, P.; Schaefer, N.; Delage, J.; Prior, J.O. Head and neck tumors angiogenesis imaging with  $^{68}\text{Ga}$ -NODAGA-RGD in comparison to 18F-FDG PET/CT: A pilot study. *EJNMMI Res.* **2020**, *10*, 47. [[CrossRef](#)] [[PubMed](#)]
26. Gnesin, S.; Mitsakis, P.; Cicone, F.; Deshayes, E.; Dunet, V.; Gallino, A.F.; Kosinski, M.; Baechler, S.; Buchegger, F.; Viertl, D.; et al. First in-human radiation dosimetry of  $^{68}\text{Ga}$ -NODAGA-RGDyK. *EJNMMI Res.* **2017**, *7*, 43. [[CrossRef](#)] [[PubMed](#)]
27. Minamimoto, R.; Karam, A.; Jamali, M.; Barkhodari, A.; Gambhir, S.S.; Dorigo, O.; Igaru, A. Pilot prospective evaluation of  $^{18}\text{F}$ -FPPRGD<sub>2</sub> PET/CT in patients with cervical and ovarian cancer. *Eur. J. Nucl. Med. Mol. Imaging* **2016**, *43*, 1047–1055. [[CrossRef](#)] [[PubMed](#)]